

Optical and electrical properties of niobium carbide

C. Y. Allison* and F. A. Modine

Solid State Division, Oak Ridge National Laboratory, Oak Ridge, Tennessee 37831

R. H. French

Department of Materials Science and Engineering, Massachusetts Institute of Technology, Cambridge, Massachusetts 02139

(Received 20 August 1986)

The optical and electrical properties were measured for single crystals of NbC_x for $x = 0.98, 0.87,$ and $0.76,$ and for one hot-isostatically-pressed sample of $\text{NbC}_{0.88}$. Specular reflectance was measured between 0.025 and 11 eV, and ellipsometry measurements were made at 1.96 eV. By using the phase obtained from ellipsometry data to correct the Kramers-Kronig analyses of the reflectances, we were able to improve the accuracy of the resulting optical functions. For energies below 6.5 eV, there are differences in the reflectance and optical functions of the samples which are due to differences in x . We interpret the low-energy optical data in terms of intraband transitions, which allows us to calculate the dc conductivity as well as other electronic transport parameters. These parameters agree well with the electrical conductivities and the Hall coefficients obtained by the van der Pauw technique. The higher-energy optical data are interpreted in light of recent electronic-structure calculations, which suggest that most interband transitions occur near the square face of the Brillouin zone.

I. INTRODUCTION

The transition-metal carbides of groups IV and V are characterized by extreme hardness, high melting points, chemical inertness, and a large number of carbon vacancies.¹⁻⁴ These materials can accommodate up to about 50% vacancies on the carbon sublattice and still retain their cubic (NaCl) structure. The number of vacancies has an enormous effect on almost all of the physical properties of these materials. These carbides have been studied by a variety of techniques, but, as a result of a scarcity of well-characterized single-crystal samples, many of these studies were done on polycrystalline samples of a single composition. Such studies cannot differentiate between properties particular to a given carbide and those particular to a given composition. For example, the reflectance spectra⁵⁻⁷ reported for TaC and ZrC are surprisingly different, given that these materials are in many other ways quite similar, and reflectances measured on the TiC system by different investigators are often very different.⁸⁻¹¹ In the present study of the niobium carbide system, whose optical properties have not been previously reported in the literature, we were fortunate to obtain several single-crystal samples of widely varying stoichiometry.

The electronic band structure of the transition-metal carbides has been of long-standing interest.^{12,13} Several of the theoretical calculations have dealt with the effect of vacancies on the electronic structure of the substoichiometric materials;¹⁴⁻²⁰ the most recent of the calculations predict vacancy states to occur near the Fermi energy. In this paper we compare our optical data to the predictions of the electronic-structure calculations, including the prediction of vacancy states.

The optical properties of metals in the infrared are dominated by the intraband transitions of free carriers. In the low-energy limit, then, the Drude model can be ap-

plied to give values for the electronic transport parameters: the dc conductivity σ , the relaxation energy γ , and the unscreened plasma frequency ω_p . In this paper we compare these parameters to those obtained from electrical measurements (conductivity and Hall coefficient) as a check on the consistency of the optical and electrical results. The electrical measurements, which give information about the number of free carriers, are also interpreted in light of the predictions of electronic-structure calculations.

II. EXPERIMENTAL ASPECTS

Three single crystals of NbC_x were examined. The first, $\text{NbC}_{0.98}$, was obtained from H. G. Smith of Oak Ridge National Laboratory, who purchased it from Alpha Crystals. A single crystal of $\text{NbC}_{0.87}$ was grown by Walter Precht of Martin Marietta and supplied by R. F. Davis of North Carolina State University. A sample of $\text{NbC}_{0.76}$ was supplied by Wendell S. Williams of the University of Illinois. A fourth sample, a polycrystalline hot-isostatically-pressed (HIP) sample of $\text{NbC}_{0.88}$ prepared by Davis was also examined. These crystals had been studied previously, and their stoichiometries were determined by lattice-parameter measurements or chemical analysis.^{21,22} The $\text{NbC}_{0.98}$ crystal had the lavender tint of nearly stoichiometric niobium carbide.

Slices approximately 1 mm thick were cut from the single-crystal boules. The samples were approximately circular, with diameters varying from 0.6 to 1 cm. They were mechanically polished with diamond grits as fine as $0.25 \mu\text{m}$, then electropolished to remove surface damage. The electrolyte was a 5:1 solution by volume of methanol and (70%) sulfuric acid. The solution was held at ~ 200 K by a dry-ice-acetone bath, and stainless steel was used as a cathode. The best conditions for an electropolish

occur just after the current peak on the I - V curve. The current peaked at about 50 mA/cm², and dropped to 10 mA/cm² at a slightly higher voltage. A five-second electropolish at the lower current caused the reflectance to drop in the ultraviolet (4–6 eV). A subsequent light mechanical polish of a few seconds with 0.25 μm diamond paste was found to increase the uv reflectance by 5% to 10% over that measured after the initial mechanical polish. This was our most successful method of sample preparation: a mechanical polish, followed by a short electropolish, following by a very light final mechanical polish. All data reported in this paper were obtained from surfaces prepared in this way.

A qualitative classification of surface roughness was given by Bennett and Porteus.²³ If an approximately Gaussian height distribution is assumed, and if the surface is relatively smooth, then the reflectance of a material at normal incidence is given by

$$R_s = R_0 \exp[-(4\pi\sigma/\lambda)^2], \quad (1)$$

where R_s is the observed reflectance, R_0 is the reflectance of a perfectly smooth surface of the same material, σ is the rms surface roughness, and λ is the wavelength of the incident light. We found that ratios of the reflectance spectra of the variously polished samples gave the exponential dependence expected, and that the samples that were mechanically polished, electropolished, and then lightly mechanically polished had the lowest surface roughness.

Reflectance measurements between 0.5 and 6.5 eV were made with a Cary Model 17D spectrophotometer equipped with a sample compartment for reflectance measurements. Because the samples were too small to be measured with the Cary V-W absolute reflectance attachment, an attachment manufactured by Harrick Scientific Corporation was used to measure the reflectance relative to an aluminum standard, purchased from the National Bureau of Standards (NBS). NBS provided a reflectance spectrum for this energy range certified to be accurate to within 0.005. Reflectances between 0.025 and 0.62 eV were measured using a Perkin-Elmer Model 983 spectrophotometer equipped with a reflectance accessory made for the instrument. This reflectance was also measured relative to aluminum. The reflectance of aluminum below 0.5 eV was taken from a collation of measurements of aged aluminum from several investigators collected by Smith, Shiles, and Inokuto.²⁴ The error in the resulting reference spectrum is judged to be $\Delta R < 0.005$. Considerable care was taken to ensure that the sample and the aluminum reference were measured through the same aperture and at the same angle of incidence. Both spectrophotometers were interfaced to a Hewlett-Packard model No. 9825 desktop computer, which facilitated data manipulation and averaging of spectral scans. The accuracy of the final results is estimated at $\Delta R < 0.02$ and probably < 0.01 over most of their range. The agreement between the two spectrophotometers in their region of overlap was very good.

Reflectance measurements were taken in vacuum from 4.5 to 11 eV with use of custom Acton Research Corporation spectrophotometer consisting of a hydrogen ioniza-

tion lamp, a 0.2-m Seya-Namioka monochromator, a dual-beam reflectometer, and sealed LiF-windowed detectors.²⁵ Because of the small size of the NbC samples, high-quality spectra were taken only on the NbC_{0.87} and NbC_{0.76} samples, where the energy resolution was 0.1 eV and the error in R was 0.10. No dramatic differences were observed in the vacuum ultraviolet (VUV) spectra of these samples. The VUV results were fitted to the more accurate results from the Cary spectrophotometer by using the 4.5- to 6.5-eV overlap region and by rigidly shifting the VUV results (down 0.04 in R for NbC_{0.87}, up 0.06 in R for NbC_{0.76}) to agree with the results from the Cary spectrophotometer.

Ellipsometry was done at one photon energy. This gave us the phase at one energy, which in the subsequent Kramers-Kronig analysis allowed us to correct the phase error introduced by a rough extrapolation of our reflectance spectra to infinite energy. This measurement was made with a Gaertner model No. L117 ellipsometer, which was equipped with a helium-neon laser of wavelength 632 nm. Measurements were made at three angles of incidence: 30°, 50°, and 70°. All three measurements gave very consistent results, the reflectances thus obtained all being within a few tenths of a percent of the values measured with the Cary spectrophotometer. We estimate that the corrected phase is accurate to within a degree in the visible and the infrared. It is less accurate in the ultraviolet, where we are approaching the limits of our data, especially for NbC_{0.98} and NbC_{0.76}, whose VUV reflectance data are less accurate because of small sample sizes.

Measurements of the dc electrical resistivity and the Hall coefficient were made by the method of van der Pauw.^{26,27} Electrical contact was made by means of platinum pins clamped to the edges of the carefully cleaned samples. Errors introduced by finite contact sizes were found to be small compared to errors caused by variations in sample thickness. The error should thus be proportional to these variations in thickness, which we estimated to be less than 5% for all samples measured. The van der Pauw measurement sequence was automated using a Hewlett-Packard 3494A scanner controlled by a Hewlett-Packard 9825 computer. Voltage measurements were made with a Keithley 181 nanovoltmeter, also controlled by the computer. Resistivity measurements showed noise in the fourth significant figure. Hall-effect voltages were of the same order as the noise and required on the order of a hundred measurements to provide adequate statistics for determining the Hall coefficient. Resistivity measurements were made with the sample mounted in a Helitran refrigerator, which gave temperature control to within 1 K between liquid-helium and room temperature.

III. RESULTS AND DISCUSSION

At low photon energies, where the Drude theory applied, one expects the following type of behavior in the reflectance spectra of typical metals. At very low energies, the spectrum should show Hagen-Rubens behavior, i.e., $1 - R \sim \sqrt{E}$.²⁸ At energies higher than this, but still below the screened plasma energy, the reflectance should be independent of energy, exhibiting a Dingle plateau.

Near the screened plasma energy, the spectrum should drop off precipitously. Looking at the reflectance spectra of NbC_x in Fig. 1, we see that only in the nearly stoichiometric case ($\text{NbC}_{0.98}$) does the reflectance show a hint of a Dingle plateau. For the more nonstoichiometric cases, the reflectance drops off rapidly at low energies. The most carbon deficient of the samples ($\text{NbC}_{0.76}$) shows the most precipitous drop in reflectance below 0.5 eV. The $\text{NbC}_{0.87}$ does not drop off as quickly, and the HIP sample, which has almost the same composition as the $\text{NbC}_{0.87}$ ($x=0.88$), has an almost identical reflectance spectrum (for this reason it is not shown in Fig. 1). Thus, increasing the vacancy concentration systematically pulls down the low-energy reflectance.

There are at least four possible causes for this systematic behavior with increasing vacancy concentration: First, the increased vacancy concentration causes a decrease in both the dc conductivity and the carrier relaxation time, since the electrons have more defects from which to scatter. Second, it may shift the Fermi level, changing the number of carriers and the plasma frequency. Third, it may broaden the interband transition, resulting in more states at low energies. Fourth, it may provide new electronic states (vacancy states) near the Fermi energy, thus creating new optical transitions at low energies.

In order to examine these various possibilities, we must distinguish the intraband contributions to the optical functions from the interband. To this end, we will discuss the intraband transitions, first by way of the electrical data in Sec. III A, then by the optical data in Sec. III B. We will concentrate on the interband transitions in Sec. III C, and in Sec. III D we will discuss the implications of defect states on our results.

A. Electronic transport measurements

The resistivity from liquid helium to room temperature of NbC of all three compositions was measured, and the results of $\text{NbC}_{0.98}$ are shown in Fig. 2. It has been found empirically^{7,21} that the resistivity of carbides can be fitted

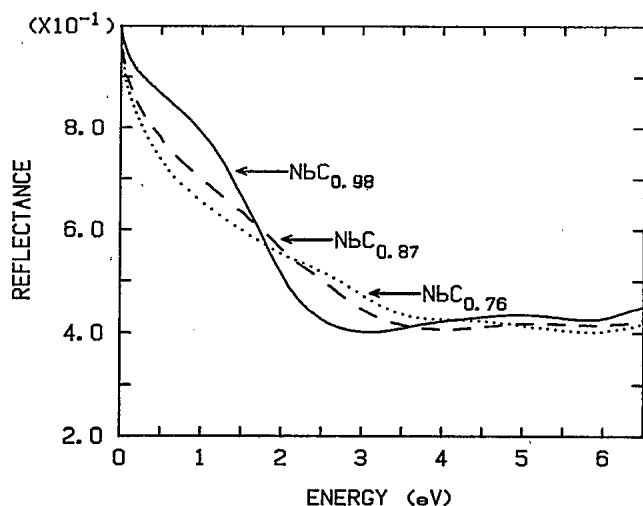


FIG. 1. Reflectance of NbC_x . Solid line: $\text{NbC}_{0.98}$; dashed line: $\text{NbC}_{0.87}$; dotted line: $\text{NbC}_{0.76}$.

TABLE I. Parameters fitted to the electrical data for niobium carbide. The Hall coefficient is computed from a Gaussian curve fitted to the measurements. The resistivity at 300 K is included for quick reference. The resistivity of $\text{NbC}_{0.76}$ is almost constant with temperature.

Parameter	$\text{NbC}_{0.98}$	$\text{NbC}_{0.87}$	$\text{NbC}_{0.76}$
ρ_0 ($\mu\Omega$ cm)	24.0	121.6	153.4
A ($\mu\Omega$ cm/K)	0.022	0.005	
B ($\mu\Omega$ cm)	22.9	9.5	
T_0 (K)	278	474	
$\rho(300$ K) ($\mu\Omega$ cm)	39.5	125.1	155.2
R_H (mm^3/C)	-0.084	-0.137	-0.026

to the following equation:

$$\rho(T) = \rho_0 + AT + B \exp(-T_0/T). \quad (2)$$

The exponential term is required to fit the bulge in the resistivity curve at intermediate temperatures, and may be interpreted as arising from a thermally activated scattering mechanism. This equation has been applied previously to niobium carbide by Dy and Williams.²¹ The solid line in the plot of resistivity in Fig. 2 is a least-squares fit of this equation. The resistivities of the other compositions of NbC_x ($x=0.87$ and 0.76) are nearly constant over the temperature range studied, and so are not shown. The parameters deduced from the fit of Eq. (1) to the resistivities of all our samples are given in Table I. These parameters are not given for the HIP sample, whose resistivity is nearly identical to that of the single-crystal $\text{NbC}_{0.87}$ sample. Our results agree well with the work of other investigators, for example, the unordered niobium carbide by Dy and Williams²¹ and the values quoted by Toth.² Our sample of $\text{NbC}_{0.76}$, which was obtained from Dy and Williams, never varied from their resistivity values by more than 2% from 4.2 to 300 K.

The most important factor influencing the resistivity is

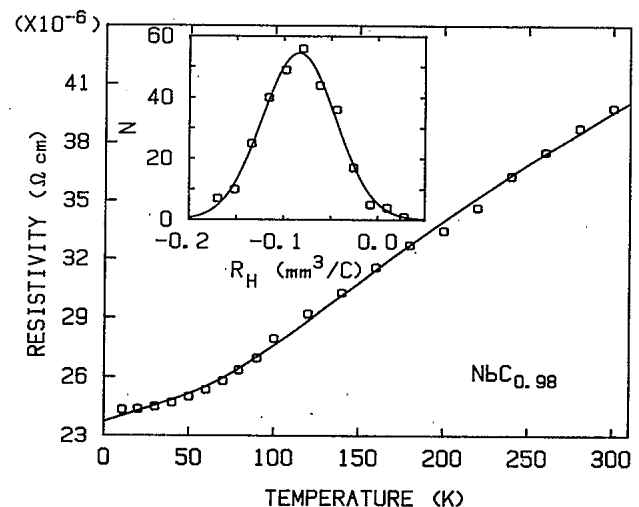


FIG. 2. Resistivity of $\text{NbC}_{0.98}$ as a function of temperature. Data fitted to Eq. (2). Inset: Hall coefficient measurements of $\text{NbC}_{0.98}$.

vacancy concentration: the residual resistivity of $\text{NbC}_{0.98}$ is $24.0 \mu\Omega \text{ cm}$, as compared to $121.6 \mu\Omega \text{ cm}$ for $\text{NbC}_{0.87}$. Even for low vacancy concentrations, however, the linear temperature coefficient is quite small compared to that of a normal metal.

The Hall coefficients at room temperature for the three compositions of the single crystals are included in Table I. We found the magnitude of the Hall coefficient to be largest for $\text{NbC}_{0.87}$ ($-0.137 \text{ mm}^3/\text{C}$) and smallest for $\text{NbC}_{0.76}$ ($-0.026 \text{ mm}^3/\text{C}$). $\text{NbC}_{0.98}$ was intermediate with a value of $-0.084 \text{ mm}^3/\text{C}$. The Hall coefficient of the HIP sample was nearly identical to that of the single-crystal $\text{NbC}_{0.87}$ sample. Since the composition of these two samples is almost the same and their electrical and optical properties are nearly indistinguishable, we will exclude further mention of the HIP sample from the following discussions.

The negative values of the Hall coefficient indicate that electrons are the predominant carriers, a conclusion supported by all previous investigations of niobium carbide. We found rough agreement with the results of earlier investigators (around $-0.1 \text{ mm}^3/\text{C}$ for nearly stoichiometric NbC quoted by Toth² and by Borukhovich *et al.*²⁹). Borukhovich *et al.*, however, found the Hall coefficient to be largest near stoichiometry, the trend found for several other carbide systems.

As a check on our data, we measured the Hall coefficient of V_8C_7 and compared it with the measurements of Shacklette and Ashworth.³⁰ This material was used because the resistivity of the ordered phases of vanadium carbide is a very sensitive function of carbon content, and we could be sure of measuring a sample of equal composition by checking the resistivity. Our sample had a room-temperature resistivity of $33.2 \mu\Omega \text{ cm}$, compared with 33.6 for Shacklette's sample. We found a Hall coefficient of $-0.17 \text{ mm}^3/\text{C}$, compared to Shacklette's value of -0.19 . This result, along with many consistent repetitions of our original measurements, gives us confidence in our values. We also note that the values of Borukhovich agree only very roughly with Shacklette's values for vanadium carbide.

If a single electronic carrier is assumed to predominate, we find additional confirmation of our Hall results in both theoretical calculations and experiments. Marksteiner *et al.*^{19,20} in a recent Korringa-Kohn-Rostoker-coherent-potential-approximation (KKR-CPA) calculation found that in both niobium carbide and vanadium carbide, the density of states (DOS) at the Fermi level reaches a minimum at compositions near $x=0.85$, in rough agreement with our maximum in the Hall coefficient at $x=0.87$. Experimental evidence supporting our Hall data is provided by the electronic specific-heat coefficients given by Toth² that imply the DOS at the Fermi level decreases with increasing vacancy concentration from $x=0.98$ to 0.83 and is nearly constant for smaller values of x . Further experimental support for our Hall data can be deduced from the optical results that are described below.

Table I shows that the resistivity curves become flatter for higher vacancy concentration, i.e., the temperature dependence becomes even smaller for the non-

stoichiometric samples. Williams attributes this effect to variations in the Hall coefficient with carbon-to-metal ratio x .¹ The resistivity depends on the product of the carrier concentration n and the mobility of the carriers. Matthiessen's rule gives this mobility as the sum of two terms: one corresponding to vacancy scattering, and the other to phonon scattering, i.e.,

$$\rho(x, T) = R_H(x, T) [1/\mu_0 + 1/\mu(T)], \quad (3)$$

where $R_H(x, T)$ is the Hall coefficient (which may be a function of both stoichiometry and temperature), μ_0 the mobility corresponding to vacancy scattering, and $\mu(T)$ corresponding to phonon scattering.

One can see from Eq. (3) that variations in R_H can change the size of the phonon scattering contribution. If R_H is independent of temperature, and $\mu(T)$ is inversely proportional to temperature, then the temperature coefficient of the resistivity is proportional to R_H . The Hall coefficient of tantalum carbide, for example, which is nearly temperature independent, increases rapidly with increasing x , and so does its temperature coefficient.³¹ In this way, Williams explains the flattening of the resistivity curves with increasing vacancy content. However, our Hall data on niobium carbide do not show such a trend of increasing Hall coefficient with x . It may be that vacancy scattering has a more complicated temperature dependence, or that the simple relation between the Hall coefficient and carrier concentration does not hold in these materials. We will present evidence in the next section that indicates that a two-carrier model may be necessary. It is also possible that a complicated temperature dependence may make this simple analysis unproductive.

The electrical data allow us to compute the dc conductivity σ , the relaxation energy γ , and the unscreened plasma frequency ω_p . Only σ is found directly from the resistivity, but γ and ω_p are related to σ by the following equation:

$$4\pi\sigma\gamma = \omega_p^2 = 4\pi Ne^2/m, \quad (4)$$

where N , e , and m are the electron concentration, charge, and effective mass, respectively. By assuming a single carrier, the carrier concentration N can be found from the Hall coefficient R_H :

$$R_H = -1/Nec. \quad (5)$$

If a free-electron mass is assumed, ω_p and γ can be estimated from N and Eq. (4). Using this we compare σ , γ , and ω_p for the three samples of NbC, and we placed them in Table II alongside the values obtained from the optical measurements discussed in the next section.

B. Intraband contributions

Here we compare our measurements of the electrical properties with the low-energy optical properties. Band-structure calculations show that most states near the Fermi energy have d symmetry.²⁶ Since the dipole selection rule does not allow transitions between states of like symmetry, interband transitions are weak at low energies, and we expect the optical properties to be dominated by intra-

TABLE II. Comparison of optical and electrical parameters for three compositions of NbC_x. Values for NbC_{0.98} were obtained from combining results of a two-carrier model (Table III).

Parameter (eV)	NbC _{0.98}		NbC _{0.87}		NbC _{0.76}	
	Optical	Electrical	Optical	Electrical	Optical	Electrical
$\hbar\omega$	13.0 ± 0.2	14.9 ± 0.7	4.6 ± 0.1	4.7 ± 0.2	3.4 ± 0.2	3.8 ± 0.2
$\hbar\gamma$	0.37 ± 0.15	0.56 ± 0.15	1.0 ± 0.5	1.1 ± 0.1	3.1 ± 1.5	7.0 ± 0.5
$\hbar\omega_p$	7.8 ± 2.0	10.2 ± 2.5	7.6 ± 2.0	8.0 ± 1.0	11.6 ± 3.0	18.3 ± 1.0

band transitions of free carriers.

We need both the reflectance and the phase of the reflected light. To get the phase, we performed a Kramers-Kronig inversion on the reflectance as described in Sec. II; the reflectance and the resulting phase out to 11 eV is shown for NbC_{0.87} in Fig. 3.

If interband transitions are negligible, if we assume a single carrier, and if we are looking at energies much lower than the screened plasma frequency ω_s , we can use the following approximations to relate the reflectance and phase to the Drude parameters:²⁸

$$(\ln R)^2/4\omega = [(1 + \omega^2/\gamma^2)^{1/2} - \omega/\gamma]/(2\pi\sigma) \quad (6)$$

and

$$\theta^2/\omega = [(1 + \omega^2/\gamma^2)^{1/2} + \omega/\gamma]/(2\pi\sigma), \quad (7)$$

where R is the reflectance, θ is the phase, σ is the dc electrical conductivity, γ is the relaxation energy (which is inversely proportional to the relaxation time τ) of the single carrier, and ω is the photon frequency. We have fitted the reflectance and phase of our three samples of niobium carbide to these equations at low energies, and we show the results for NbC_{0.87} in Fig. 4 and for NbC_{0.98} in Fig. 5.

Examination of Eqs. (6) and (7) shows that the y intercept, since it determines the value of σ , should be the same for both the reflectance and the phase of a given sample. Also, the slopes near zero energy of both quantities should be equal in magnitude but opposite in sign. For NbC_{0.76} and for NbC_{0.87}, both these expectations hold true (see Fig. 4 for $x=0.87$). However, for the NbC_{0.98}

sample, the fits of the reflectance and the phase do not meet at 0 eV, and the low-energy slopes are not equal in magnitude. It is clear that Eqs. (6) and (7) will never give a consistent value for the dc conductivity or the relaxation energy for this sample.

Alternatively, we can determine the Drude parameters by fitting other optical functions. Once both the reflectance and the phase are known, the optical constants and the dielectric functions can be computed by use of the following well-known relations:

$$re^{i\theta} = (n + ik - 1)/(n + ik + 1) \quad (8)$$

and

$$\epsilon_1 + i\epsilon_2 = (n + ik)^2, \quad (9)$$

where $r = \sqrt{R}$ is the reflectance amplitude, n and k are the real and imaginary parts of the index of refraction, and ϵ_1 and ϵ_2 are the real and imaginary parts of the dielectric functions. The dielectric function for NbC_{0.87} is shown in Fig. 6. The optical conductivity is related to the dielectric function as follows:

$$\sigma_1 = \omega\epsilon_2/4\pi \quad (10)$$

and

$$\sigma_2 = (\omega/4\pi)(1 - \epsilon_1), \quad (11)$$

where σ_1 and σ_2 are the real and imaginary parts of the optical conductivity. The optical conductivities are convenient, because the dc conductivity can be estimated by

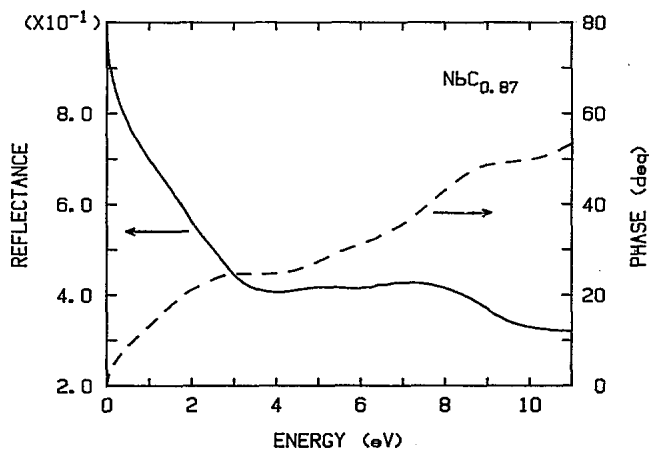


FIG. 3. Reflectance (solid line) and phase (dashed line) of NbC_{0.87}.

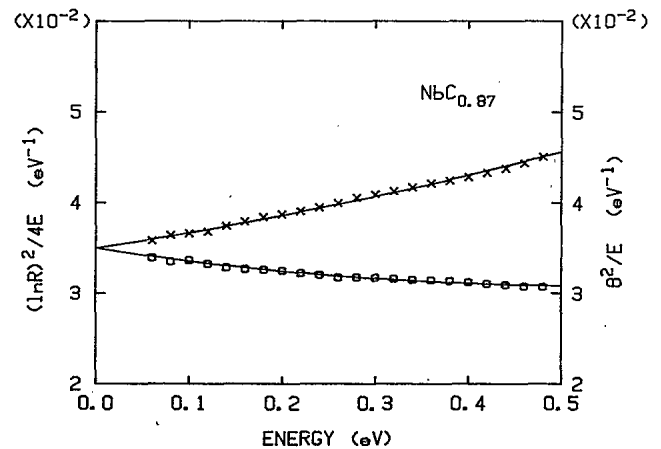


FIG. 4. Reflectance (squares) and phase (crosses) of NbC_{0.87} fitted to Eqs. (6) and (7), respectively.

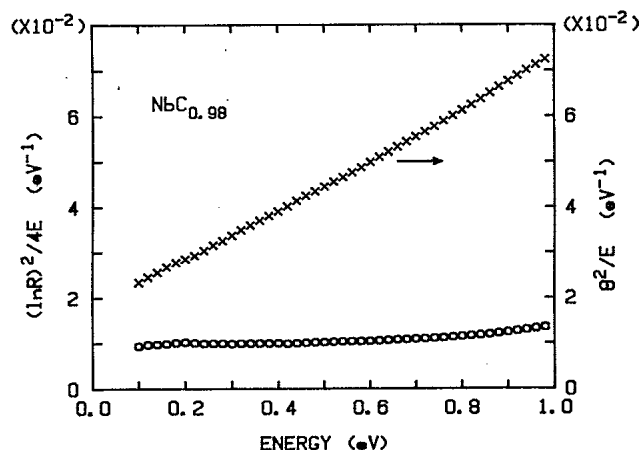


FIG. 5. Reflectance (squares) and phase (crosses) of $\text{NbC}_{0.98}$.

extrapolation of the real part of the conductivity to zero energy, and the relaxation energy is the energy of the lowest-energy peak of σ_2 .⁷ Alternatively, the functions can be fitted to the Drude theory to give more accurate values of the relaxation energy and the plasma frequency.^{7,28} The optical conductivities for the three samples of NbC are given in Figs. 7, 8, and 9.

The Drude model gives a good fit to the optical conductivity in the cases of $\text{NbC}_{0.76}$ and $\text{NbC}_{0.87}$, if interband transitions at low energies are taken into account (the method of doing so is discussed in the next section). However, in the case of $\text{NbC}_{0.98}$, good agreement with the data cannot be obtained with reasonable values of both the dc conductivity and the relaxation energy. The difficulties in fitting the data for this sample suggests that our assumption of a single carrier is not valid, at least for the case of $\text{NbC}_{0.98}$. In fact, a single-carrier model appears to be inadequate for all the group-V carbides. Earlier work indicates that a single carrier cannot explain the Hall coefficients of vanadium carbide³⁰ and tantalum carbide,³¹ nor the optical data of tantalum carbide.⁶ On the other

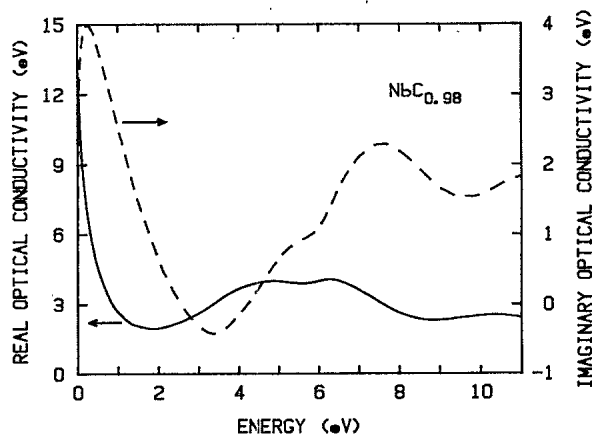


FIG. 7. Real (solid line) and imaginary (dashed line) parts of the optical conductivity of $\text{NbC}_{0.98}$.

hand, our earlier work on zirconium carbide⁷ and titanium carbide, both of which are in group IV, was explained without the need to introduce a second carrier.

On the strength of this evidence, we examined a fit of the low-energy optical conductivity to a two-carrier conductivity just as was done in earlier work on tantalum carbide.⁶ The sum of the resulting two conductivities (5.8 and 7.2 eV) is close to the electrical value (14.9 eV), and the fit to the low-energy optical conductivity is much better. This fit of the optical conductivity from 0 to 1 eV is shown in Fig. 10, and the Drude parameters obtained in the fit are summarized in Table III.

Despite the difficulties, the Drude theory works reasonably well. The dc conductivity agrees quite well with the zero-energy optical conductivity in all cases: for $x=0.98$, 14.9 eV compared to 13.0 eV (optical); for $x=0.87$, 4.7 eV compared to 4.6 eV; and for $x=0.76$, 3.8 eV compared to 3.4 eV. The other parameters, relaxation energy, and plasma frequency, were found in three ways: fitting Eqs. (6) and (7), measuring the energy of the lowest-energy peak in σ_2 , and fitting the optical conductivities by the

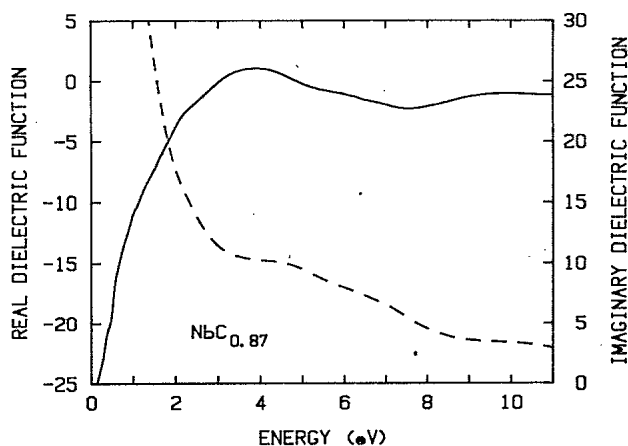


FIG. 6. Real (solid line) and imaginary (dashed line) parts of the dielectric function of $\text{NbC}_{0.87}$.

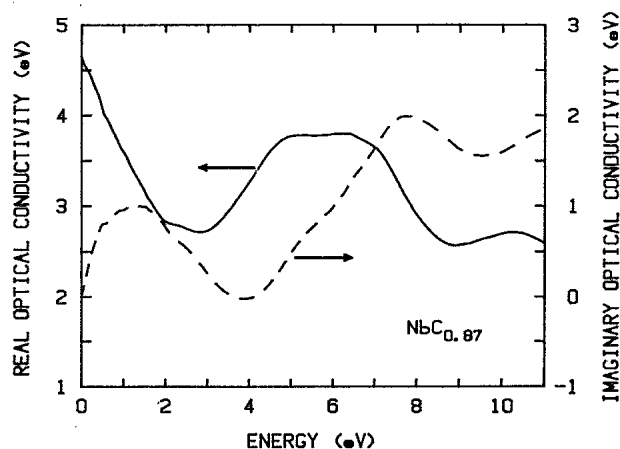


FIG. 8. Real (solid line) and imaginary (dashed line) parts of the optical conductivity of $\text{NbC}_{0.87}$.

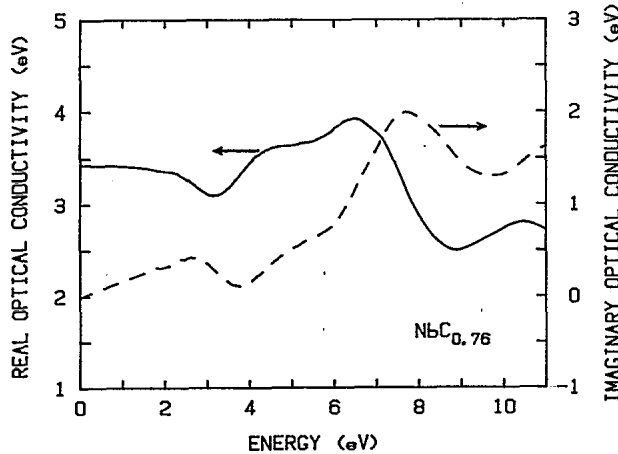


FIG. 9. Real (solid line) and imaginary (dashed line) parts of the optical conductivity of $\text{NbC}_{0.76}$.

Drude theory. These parameters are more difficult to obtain than the dc conductivity, since interband transitions at low energies will obscure them. In fitting the optical conductivities by the Drude theory, we have taken the interband transitions into account at least roughly by methods described below. Values spanning the range of the results obtained by these three techniques are compiled in Table II. Although the agreement of these parameters is rather crude, especially for the non-stoichiometric cases (the electrical values are consistently higher than the optical values), similar trends are seen: increasing relaxation energy with vacancies and a maximum in the plasma frequency at $x=0.87$. We consider the agreement to be good, considering the assumptions and difficulties that are inherent in the analyses.

C. Interband contributions and band structure

In this section we compare our optical conductivities and interpret them in light of recent band-structure calculations. First we note that the real part of the optical con-

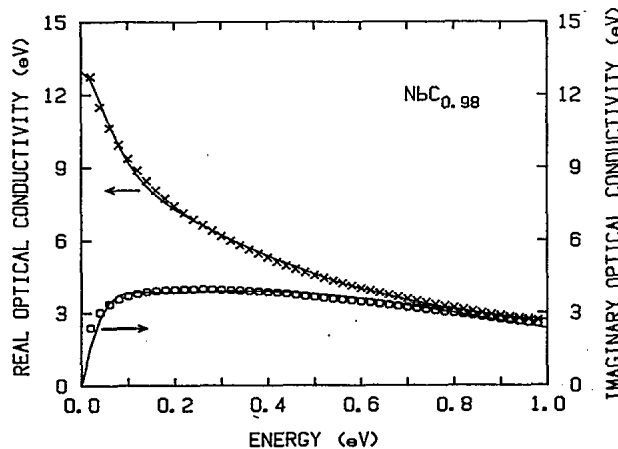


FIG. 10. Fit of optical conductivity to a two-carrier model. Squares: real part. Crosses: imaginary part.

TABLE III. Fit of low-energy (<1 eV) optical conductivity of $\text{NbC}_{0.98}$ to a two-carrier model.

Parameter (eV)	Carrier 1	Carrier 2	Combined
$\hbar\sigma$	5.8	7.2	13.0
$\hbar\gamma$	0.078	0.75	0.37
$\hbar\omega_p$	2.4	7.4	7.8

ductivity is related to the density of states. The real part of the optical conductivity can be expressed as³²

$$\sigma_1(E) = (1/E)(e^2\hbar^3/m^2V) \sum_{k,k'} |\langle \psi_{k'} | (\partial/\partial x) | \psi_k \rangle|^2 \times \delta(\epsilon_{k'} - \epsilon_k - E). \quad (12)$$

If we assume constant matrix elements, the summation over the energy-conserving δ function becomes an integral over the density-of-states function $N(E)$, i.e.,

$$\sigma_1(E) \sim (1/E) \int_{E_F}^{E_F+E} N(E')N(E'-E)dE'. \quad (13)$$

Comparison of the optical conductivity calculated from Eq. (13), using the densities of states given by the various band-structure calculations, and our experimental optical conductivity gives us a test of the band structures, assuming intraband effects can be taken into account. In a perfect crystal, however, the matrix elements are zero unless both initial and final states have the same wave vector, i.e., only vertical transitions are allowed for optical transitions. We use Eq. (13), which neglects the k -selection rule, for computational simplicity. Since k is not a good quantum number in a disordered crystal, this simplification has some justification in the substoichiometric case. However, we expect no more than qualitative agreement with experiment.

We applied this technique to the linear combination of atomic orbital-coherent potential approximation calculations of Klein, Papaconstantopoulos, and Boyer.¹⁴ They found densities of states (DOS) for NbC_x with $x=0.7, 0.8, 0.9$, and 1.0 . They also showed the partial DOS for the carbon s and p and the niobium d states, which allowed us to include the dipole selection rule (i.e., we only considered transitions of the type p to d and s , and d and s to p).³² The resulting optical conductivity, using the data of Klein *et al.* for $\text{NbC}_{1.0}$, are given in Fig. 11. The calculation predicts a peak at about 8 eV primarily due to transitions from the p -like carbon peak below the Fermi level to the d -like niobium peak above it.

We also found the optical conductivity from the DOS given by the tight-binding calculation of Pecheur *et al.*¹⁸ Here we did not include the effects of the dipole selection rule since only the total density of states was given. Figure 11 shows the results for two compositions of NbC_x : $x=1.0$ and 0.90 . We see the carbon p -state to niobium d -state peak at 7 eV in this calculation. The larger conductivity at low energies is due to the neglect of the dipole selection rule.

It would be interesting to compare with this an optical

conductivity calculated from the DOS of Marksteiner *et al.*^{19,20} Unfortunately, their DOS extend only 1.2 eV above the Fermi energy. Thus, an optical conductivity cannot be computed for energy above 1.2 eV from their results.

The main features in our experimental optical conductivity spectra, the peaks at 5 and 7 eV, agree well with the calculated optical conductivities. The 7-eV peak corresponds to the p to d transitions mentioned above. Although the calculated conductivities are qualitatively very similar, the peak at 7 eV agrees better with the DOS of Pecheur *et al.* than with the DOS of Klein *et al.* The peak at 5 eV corresponds to a shoulder in the calculated optical conductivities, which appears to be caused by transitions from the carbon p states to the rapidly increasing number of states just below the metal d -state peak. This 5-eV peak appears to shift in energy by about half an electron volt over the composition range studied. A comparable shift is seen in the optical conductivity calculated from Pecheur's DOS.

These features in the optical conductivity come most likely from transitions between nearly parallel bands. Inspection of the band-structure diagram of stoichiometric NbC from Klein *et al.*¹⁴ reveals several parallel bands near the X , W , and K points, i.e., on the square face of the Brillouin zone. Two sets have a separation of around 8 eV, which explains the peak at that energy in the calculated optical conductivity, and others have separations of between 4 and 6 eV, energies where transitions are seen to occur. There is also one set of nearly parallel bands with an 8 eV separation at the Γ , or center, point in the Brillouin zone. The band structure of Gupta and Freeman¹² agrees very closely with that of Klein, even giving the same energy separations at the X and Γ points. The band structure of Pecheur *et al.*¹⁸ looks very similar to that of Klein on the square face of the zone boundary, except the separation between the bands is somewhat less (7 eV instead of 8 eV, for example), which agrees better with our

experimental results. The band structure of Chadi and Cohen¹³ differs substantially from the calculations listed above, and it is difficult for us to correlate it with our experimental findings. In summary, it appears that most of the optical transitions occur between parallel bands on the square face of the Brillouin zone.

D. Defect states

We found in Sec. III B that there were three possibly ways of determining ω_p and γ , each of which gave somewhat different values. In order to find these parameters, one must assume that interband transitions are not important at low energies. Recent calculations, however, show that in nonstoichiometric materials, new states are formed near the Fermi energy. If defect states contribute to optical transitions, they would make the separation between interband and intraband contributions difficult, and would thus affect the values of parameters deduced using the Drude theory.

Most of these recent calculations predict the defect states to occur within 1 or 2 eV of the Fermi energy,¹⁵⁻²⁰ and they have been verified experimentally in the transition-metal carbides by several investigators by x-ray photoemission spectroscopy (XPS) and electron-energy-loss spectroscopy (EELS).³³⁻³⁷ The effect of the defect states on the optical conductivity is shown in Fig. 11, where we see from the results of Pecheur *et al.*¹⁸ that transitions are shifted to lower energies.

It might be possible to verify the existence of these states in the present work by looking at the optical conductivities, if intraband contributions could first be subtracted out. To do so, however, one needs values of the Drude parameters, only one of which (the dc conductivity) is known to a high degree of accuracy. The others (relaxation energy and plasma energy) must be found by fitting the data in the same energy regime as the proposed defect states. Therefore, no clear separation between interband and intraband terms is possible.

One can attempt to model the low-energy (below 2-3 eV) optical conductivity by using a Lorentz oscillator to simulate the defect states along with the Drude model for the intraband contribution. The nonstoichiometric niobium carbide samples can be fitted quite well in this way. For NbC_{0.87}, for example, the relaxation energy is set at 0.5 eV, and the Lorentz oscillator at a little over 1 eV. The inclusion of the Lorentz oscillator lowers the relaxation energies, and they are given as the lower limit in Table II. The existence of low-energy defect states is thus consistent with our results, and these states probably contribute to the variations in our relaxation energies and plasma energies.

In summary, the changes in optical properties with composition are due first to lowered conductivity and relaxation time from vacancy scattering. There is probably also a contribution from transitions due to defect states at low energies. The two other possibilities mentioned earlier in this section, a shift in the Fermi energy and a broadening of the DOS, do not seem likely to cause these variations in optical properties. Most recent calculations show either no change in the Fermi energy (e.g., Pecheur

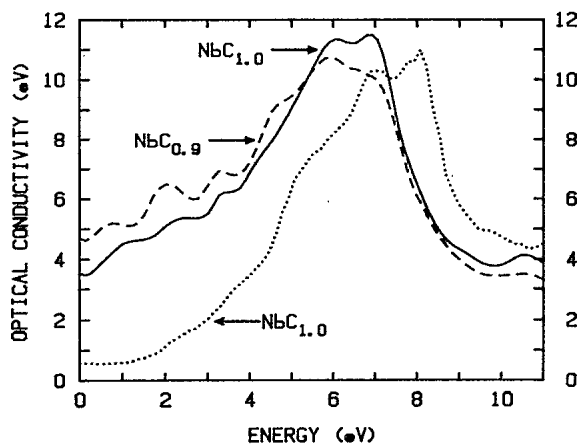


FIG. 11. Real part of optical conductivities calculated from Eq. (13). Solid line (NbC_{1.0}) and dashed line (NbC_{0.90}): density of states from Pecheur *et al.* Dotted line (NbC_{1.0}): density of states from Klein *et al.*

*et al.*¹⁸) or a downward shift with increasing vacancy concentration (e.g., Marksteiner *et al.*^{19,20}). According to all density-of-states calculations, such a downward shift will lower the number of states at the Fermi level. Thus, a shift in the Fermi energy will most likely reduce the number of states within 1–2 eV of the Fermi energy, rather than increase them, and so it will not account for the changes of optical properties with composition. It will, however, change the number of free carriers, which affects the dc conductivity and the Hall coefficient. Broadening effects in the density of states which occur with increasing vacancy content do not appear large enough from the recent calculations to play a significant role in the change in optical properties.

IV. CONCLUSIONS

Reflectance and ellipsometry have been combined to obtain the optical functions of niobium carbide of three compositions. The optical functions were compared to electrical measurements (conductivity and Hall coefficient) and recent electronic-structure calculations.

We find that the zero-energy optical conductivity and the dc electrical conductivity agree very well. The slight differences observed can easily be attributed to experimental uncertainties and to the difference between the surface (sampled by optical techniques) and the bulk (sampled by electrical measurements): The optical results are slightly lower, suggesting that the polished surface has more defects than the bulk. Good agreement between optical and electrical conductivities is seen in all the transition-metal carbides we have studied.^{6,7}

There is only fair agreement between the other Drude parameters (relaxation energy and plasma energy) obtained from electrical and optical measurements. This is to be expected, since these parameters are not measured directly, and they depend on assumptions which may not be true. For example, it is likely that transitions due to defect states are not negligible at low energies, and that they affect our values of the Drude parameters. We also assumed a single carrier in the analysis of the electrical data, which is at variance with our finding for NbC_{0.98} that a two-carrier model is better.

We have seen that the two-carrier model is required only for the NbC_{0.98} sample. Two possible explanations may be put forward. First, one of the carriers may be scattered more strongly by vacancies, making the contribution to the resistivity by the second carrier negligible at high vacancy concentrations. Another possibility is a frequency-dependent relaxation energy. One would expect the frequency-dependent part to be obscured at high vacancy concentrations by a large vacancy contribution. The addition of a term proportional to the square of the energy to the relaxation rate, however, was not nearly as successful as the two-carrier fit to the low-energy optical data.

Both the electrical and the optical measurements support the conclusion of Marksteiner *et al.*^{19,20} that the largest number of carriers occurs at intermediate ($x=0.87$) compositions. Marksteiner noted³⁸ that this result is due to two competing effects: (1) a small downward shift in the Fermi energy as x is decreased, which initially lowers the number of states, and (2) the creation of new defect states at high vacancy concentrations which eventually overwhelms the effect of the Fermi-level shift. Thus, our data are again consistent with the existence of defect states.

The main features in our optical conductivity spectra agree well with the calculated densities of states, and they can be compared qualitatively with band structure. We found that most of the optical transitions occur between nearly parallel bands that are found near the X , W , and K points (i.e., the square face of the Brillouin zone).

We also found that a hot-isostatically-pressed sample of NbC _{x} has optical and electrical properties that are almost identical to those of a single crystal with nearly the same composition. This suggests that it is possible to obtain reliable information on the properties of transition-metal carbides without using single crystals.

ACKNOWLEDGMENTS

This research was sponsored by the Division of Materials Sciences, U.S. Department of Energy under Contract No. DE-AC05-84OR21400 with Martin Marretta Energy Systems, Inc.

*Permanent address: Department of Physics, Oklahoma State University, Stillwater, OK 74074.

¹W. S. Williams, *Progress in Solid State Chemistry*, edited by H. Reiss and J. O. McCaldin (Pergamon, New York, 1971), Vol. 6.

²L. E. Toth, *Transition Metal Carbides and Nitrides* (Academic, New York, 1971).

³G. V. Samsonov, *High Temperature Materials, Properties Index* (Plenum, New York, 1964).

⁴Karlheinz Schwartz, *CRC Crit. Rev. Solid State Mater. Sci.* (to be published).

⁵J. F. Alward, C. Fong, M. El-Batanouny, and F. Wooten, *Phys. Rev. B* **10**, 1105 (1975).

⁶F. A. Modine, R. Major, T. Haywood, G. Gruzalski, and D. Y. Smith, *Phys. Rev. B* **29**, 836 (1984).

⁷F. A. Modine, T. Haywood, and C. Allison, *Phys. Rev. B* **32**,

7743 (1985).

⁸R. G. Lye and E. M. Logothetis, *Phys. Rev.* **147**, 622 (1966).

⁹D. Lynch, C. Olson, D. Peterman, and J. Weaver, *Phys. Rev. B* **22**, 3991 (1980).

¹⁰L. Roux, J. Hanus, J. Francois, and M. Sigrist, *Sol. Energy Mater.* **7**, 299 (1982).

¹¹B. Karlsson, J.-E. Sundgren, and B.-O. Johansson, *Thin Solid Films* **87**, 181 (1982).

¹²M. Gupta and A. Freeman, *Phys. Rev. B* **14**, 5205 (1976).

¹³D. Chadi and M. Cohen, *Phys. Rev. B* **10**, 496 (1974).

¹⁴B. M. Klein, D. A. Papaconstantopoulos, and L. L. Boyer, *Phys. Rev. B* **22**, 1946 (1980).

¹⁵G. Ries and H. Winter, *J. Phys. F* **10**, 1 (1980).

¹⁶L. Huisman, A. Carlsson, C. Gelatt, and H. Ehrenreich, *Phys. Rev. B* **22**, 991 (1980).

¹⁷L. Porte, L. Roux, and J. Hanus, *Phys. Rev. B* **28**, 3214

- (1983).
- ¹⁸P. Pecheur, G. Toussaint, and E. Kauffer, *Phys. Rev. B* **29**, 6606 (1984).
- ¹⁹P. Marksteiner, P. Weinberger, A. Neckel, R. Zeller, and P. Dedericks, *Phys. Rev. B* **33**, 812 (1986).
- ²⁰P. Marksteiner, P. Weinberger, A. Neckel, R. Zeller, and P. Dedericks, *Phys. Rev. B* **33**, 6709 (1986).
- ²¹L. C. Dy and W. S. Williams, *J. Appl. Phys.* **53**, 8915 (1982).
- ²²S. Chevacharopukul, R. F. Davis, and J. Peterson, *Mater. Sci. Eng.* **55**, 289 (1982).
- ²³H. E. Bennett and J. O. Porteus, *J. Opt. Soc. Am.* **51**, 123 (1961).
- ²⁴D. Y. Smith, E. Shiles, and M. Inokuti, Argonne National Laboratory Report No. 83-24, 1983 (unpublished), available from the National Technical Information Services, U.S. Department of Commerce.
- ²⁵R. H. French, Ph.D. thesis, Massachusetts Institute of Technology, Cambridge, Mass., 1985.
- ²⁶L. J. van der Pauw, *Phillips Res. Rep.* **13**, 1 (1953).
- ²⁷L. J. van der Pauw, *Phillips Tech. Rev.* **26**, 220 (1958).
- ²⁸F. A. Modine and D. Y. Smith, *J. Opt. Soc. Am. A* **1**, 1171 (1984).
- ²⁹A. Borukhovich, P. Geld, V. Tskhai, L. Dubrovskaya, and I. Matveenko, *Phys. Status Solidi B* **45**, 179 (1971).
- ³⁰L. W. Shacklette and H. Ashworth, *J. Appl. Phys.* **44**, 5254 (1973).
- ³¹G. Santoro and R. Dolloff, *J. Appl. Phys.* **39**, 2293 (1968).
- ³²W. A. Harrison, *Electronic Structure and the Properties of Solids* (Freeman, San Francisco, 1980).
- ³³G. R. Gruzalski, D. M. Zehner, and G. Ownby, *Surf. Sci.* **157**, L395 (1985).
- ³⁴G. R. Gruzalski and D. M. Zehner, *Phys. Rev. B* **34**, 3841 (1986).
- ³⁵H. Hochst, P. Steiner, S. Hufner, and C. Politis, *Z. Phys. B* **37**, 27 (1980).
- ³⁶J. Pflugger, J. Fink, W. Weber, E.-P. Bohnen, and G. Crecelius, *Phys. Rev. B* **30**, 1155 (1984).
- ³⁷J. Pflugger, J. Fink, W. Weber, K.-P. Bohnen, and G. Crecelius, *Phys. Rev. B* **31**, 1244 (1985).
- ³⁸P. Marksteiner (private communication).